AMERICAN SOCIETY FOR MICROBIOLOGY | Molecular and Cellular Biology®

RESEARCH ARTICLE

hnRNP Q Regulates Internal Ribosome Entry Site-Mediated *fmr1* Translation in Neurons

Jung-Hyun Choi,[a] Sung-Hoon Kim,[d]* Young-Hun Jeong,[a] Sung Wook Kim,[d] Kyung-Tai Min,[b,c] Kyong-Tai Kim[a,d]

[a]Department of Life Sciences, Pohang University of Science and Technology, Pohang, Republic of Korea
[b]Department of Biological Sciences, School of Life Sciences, Ulsan National Institute of Science and Technology, Ulsan, Republic of Korea
[c]National Creative Research Initiative Center for Proteostasis, Ulsan National Institute of Science and Technology, Ulsan, Republic of Korea
[d]Division of Integrative Biosciences and Biotechnology, Pohang University of Science and Technology, Pohang, Republic of Korea

ABSTRACT Fragile X syndrome (FXS) caused by loss of fragile X mental retardation protein (FMRP), is the most common cause of inherited intellectual disability. Numerous studies show that FMRP is an RNA binding protein that regulates translation of its binding targets and plays key roles in neuronal functions. However, the regulatory mechanism for FMRP expression is incompletely understood. Conflicting results regarding internal ribosome entry site (IRES)-mediated *fmr1* translation have been reported. Here, we unambiguously demonstrate that the *fmr1* gene, which encodes FMRP, exploits both IRES-mediated translation and canonical cap-dependent translation. Furthermore, we find that heterogeneous nuclear ribonucleoprotein Q (hnRNP Q) acts as an IRES-transacting factor (ITAF) for IRES-mediated *fmr1* translation in neurons. We also show that semaphorin 3A (Sema3A)-induced axonal growth cone collapse is due to upregulation of hnRNP Q and subsequent IRES-mediated expression of FMRP. These data elucidate the regulatory mechanism of FMRP expression and its role in axonal growth cone collapse.

KEYWORDS FMRP, Fmr1, IRES, hnRNP Q, neuron, translation

Fragile X syndrome (FXS) due to the absence of fragile X mental retardation protein (FMRP) is the most common inherited neurological disorder that causes intellectual disability, as well as autism (1–3). Healthy individuals have around 30 repeats of CGG in the 5′ untranslated region (UTR) of the fragile X mental retardation 1 gene (*fmr1*); however, patients with FXS have extensive expansion of the CGG repeats (>200 repeats), leading to hypermethylation (4–6). This results in transcriptional inhibition of the *fmr1* gene, which subsequently leads to an absence of FMRP. Functionally, FMRP is an RNA binding protein that regulates the translation of its target mRNA and is ubiquitously present in the brain (7–10). In *fmr1* knockout (KO) mice and FXS patients, an absence of FMRP impairs synaptic responses because its target mRNAs involved in controlling synaptic functions or structure are abnormally translated (2, 11, 12). Thus, a large number of studies have investigated the roles of FMRP in the brain; however, the regulatory mechanism of FMRP expression itself has been mostly unexplored.

During the translation of mRNA transcripts, the existence of cap structure at the 5′ end is known to be very important in recruiting ribosomes. In the traditional cap-dependent translation, the 40S ribosomal subunit is recruited to the 5′ cap structure of mRNA. The 40S subunit scans down in a 5′-to-3′ direction until the start codon is recognized, at which time the joining of large subunits (60S) occurs and protein synthesis begins (13–15). Cap-independent translation may use an internal ribosome entry site (IRES) to recruit ribosomes internally to the mRNA rather than at the 5′ end. IRES-mediated translation does not require a 5′ cap structure (16–20). It has been

Citation Choi J-H, Kim S-H, Jeong Y-H, Kim SW, Min K-T, Kim K-T. 2019. hnRNP Q regulates internal ribosome entry site-mediated *fmr1* translation in neurons. Mol Cell Biol 39:e00371-18. https://doi.org/10.1128/MCB.00371-18.

Address correspondence to Kyung-Tai Min, ktaimin@unist.ac.kr, or Kyong-Tai Kim, ktk@postech.ac.kr.

* Present address: Sung-Hoon Kim, Department of Biochemistry and Goodman Cancer Research Centre, McGill University, Montreal, Quebec, Canada.

Received 23 July 2018
Returned for modification 20 August 2018
Accepted 15 November 2018
Accepted manuscript posted online 26 November 2018
Published 24 January 2019

reported that about 10% of the human 5′ UTR contains IRES elements (21), suggesting that IRES-mediated translation plays key roles in protein synthesis.

As reported previously, these IRES elements are greatly affected by the presence of certain RNA binding proteins, also known as IRES-transacting factors (ITAFs) (22, 23). These ITAFs may enhance or suppress IRES-mediated translation through mechanisms that still remain unclear. Heterogeneous nuclear ribonucleoproteins (hnRNPs) are a group of RNA binding proteins that participate in fundamental cellular regulation, including RNA metabolism. Many of these heterogeneous nuclear ribonucleoproteins have also been found to function as ITAFs (20, 24–26). hnRNP Q, also known as SYNCRIP, is an AU-rich RNA binding protein that has multiple functions in RNA metabolism, such as pre-mRNA splicing, mRNA editing, and mRNA translation (27). Many earlier reports also confirmed its role in regulating IRES-mediated translation of cellular mRNA (24, 26, 28–32).

In neuron development, the axonal growth cone of a neuron travels over great distances to form a connection with a target, such as a dendritic spine of another neuron. In the midst of the process, the growth cone of a neuron can either collapse or extend in response to axonal guidance cues (33, 34). This event of growth cone collapse or extension is necessary in neuronal development, as it allows the neuron to make a proper connection with the correct target. Semaphorins are a family of membrane-bound proteins that function as axonal guidance cues in the brain (33, 35–37). More specifically, semaphorin 3A (Sema3A) is an axonal guidance protein that induces growth cone collapse through its activity as a neuronal repellant.

The translational mechanism behind the translation of *fmr1* mRNA became a controversial issue recently. Two previous studies reported that *fmr1* exploits IRES-mediated translation (38, 39). Using bicistronic vectors, the authors found an element that function as an IRES upstream of CGG repeats. On the other hand, another report showed a conflicting result in which FMRP was expressed only in a cap-dependent manner (40). The authors utilized hairpin insertion at the beginning of the 5′ UTR of *fmr1* mRNA to block the cap-dependent translation but were not able to detect any sign of cap-independent translation. Here, we elucidate that *fmr1* translation uses both cap-dependent and cap-independent mechanisms. Furthermore, we identify an ITAF for IRES-mediated *fmr1* translation that plays a key role in Sema3A-induced axonal growth cone collapse. Our work provides insights into the regulatory mechanism of FMRP expression and its physiological contribution during axon development.

RESULTS

FMRP expression utilizes IRES-mediated translation. Previous reports showed that the 5′ UTR of human *fmr1* contains a pyrimidine-rich region that is required for IRES-mediated translation (38, 39); however, Ludwig et al. (40) also claimed that *fmr1* translation does not utilize IRES-mediated translation and uses only a cap-dependent ribosome scanning mechanism. To clarify this discrepancy and to test whether the *fmr1* 5′ UTR contains IRES activity, we constructed a bicistronic reporter system that can distinguish cap-dependent expression (renilla luciferase [RLUC]) from cap-independent expression (firefly luciferase [FLUC]) (30). The cytomegalovirus (CMV) promoter drives the transcription of a transcript that encodes RLUC and FLUC; however, translation of FLUC depends on the IRES activity of the sequences inserted upstream of the FLUC coding region. The full-length 5′ UTR of the mouse *fmr1* gene was inserted between the stop codon of RLUC and the start codon of FLUC. The reverse form of the mouse *fmr1* gene was used as a negative control, while the encephalomyocarditis virus (EMCV) gene was used as a positive control (41). The result showed that the activity of FLUC, which is normalized by the activity of RLUC, was significantly higher with the 5′ UTR of *fmr1* than with the reverse form of the 5′ UTR of *fmr1*. Also, the activity of FLUC with the 5′ UTR of *fmr1* showed strength similar to that of the activity of FLUC with the 5′ UTR of EMCV, which is known to have cap-independent translation (Fig. 1A). We also confirmed this result with vectors that contained a simian virus 40 (SV40) promoter. The

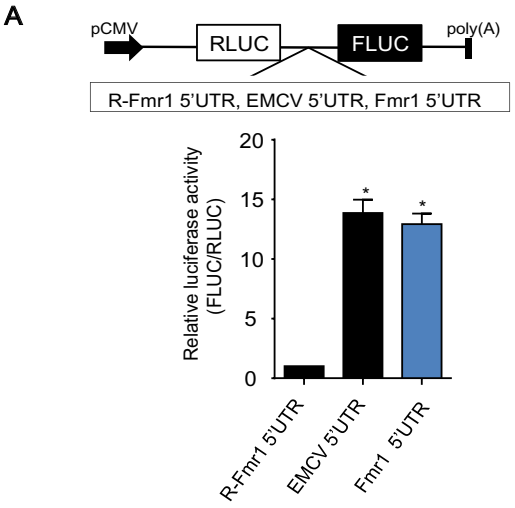

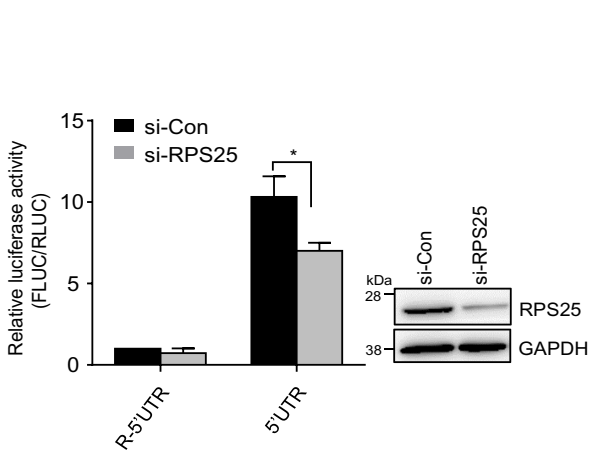

	R-Fmr1	EMCV	Fmr1
FLUC	3,932	165,919	102,894
RLUC	201,585	615,590	407,095

si-Con	R-5'UTR	5'UTR
FLUC	37,023	73,484
RLUC	1,559,017	326,687

siRPS25	R-5'UTR	5'UTR
FLUC	9,805	55,350
RLUC	612,495	387,965

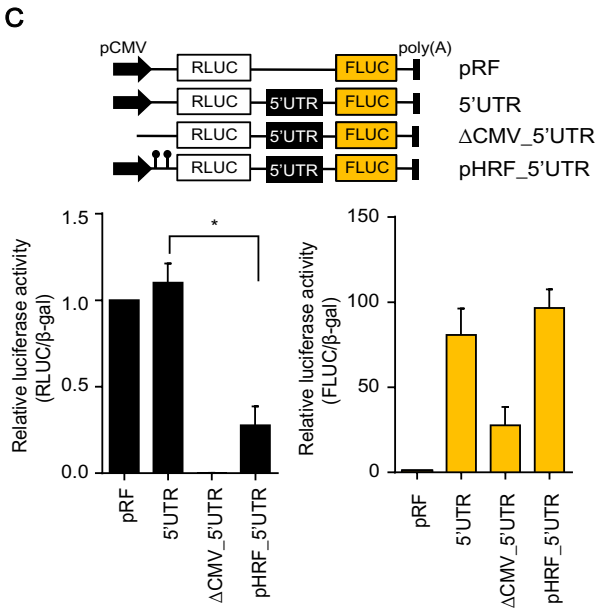

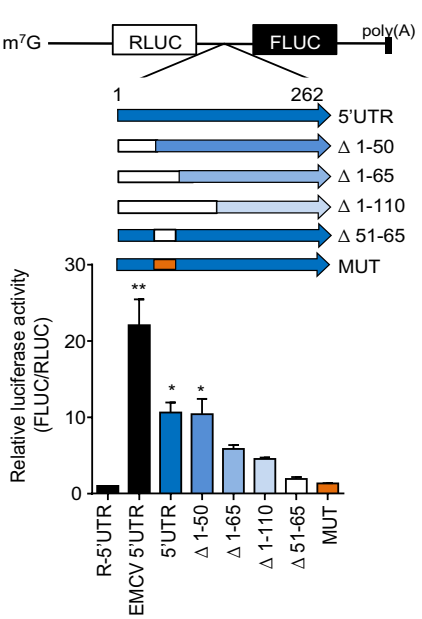

	pRF	5'UTR	ΔCMV_ 5'UTR	pHRF_ 5'UTR
FLUC	32,208	1,658,965	530,129	1,716,652
RLUC	7,955,242	5,528,138	270	835,554
β-gal	0.4007	0.2535	0.2607	0.2266

	R-5'UTR	EMCV	5'UTR	Δ 1-50
FLUC	2,322	77,960	3,484	39,251
RLUC	3,540,380	5,688,805	433,445	4,165,880

	Δ 1-65	Δ 1-110	Δ 51-65	MUT
FLUC	11,661	11,904	3,158	372
RLUC	2,643,778	3,714,443	2,472,876	476,819

FIG 1 IRES-mediated *fmr1* translation generates FMRP. (A) Neuro2A cells were transfected (24 h) with the following expression vector: pRF containing a reverse form of the *fmr1* 5′ UTR, the 5′ UTR of encephalomyocarditis virus (EMCV), and the 5′ UTR of *fmr1*. With the lysate of transfected cells, firefly and renilla luciferase activities were measured using dual-luciferase assays. The activity of FLUC was normalized by the activity of RLUC. The table contains representative raw data that were obtained using a luminometer (MicroLumatPlus). *, $P < 0.001$; $n = 5$ independent experiments. The values represent means and standard errors of the mean (SEM), and statistical significance was tested by one-way ANOVA followed by a Bonferroni *post hoc* test. (B) Neuro2A cells were transfected with either a pRF expression vector that contained a reverse form of the *fmr1* 5′ UTR or the regular form of the *fmr1* 5′ UTR (24 h) after negative control (si-Con) or si-RPS25 transfection (24 h). Dual-luciferase analyses were performed, and cell lysates were

(Continued on next page)

result showed the highest activity of FLUC with the 5′ UTR of *fmr1* (see Fig. S1A in the supplemental material).

To confirm whether the increase in the activity of FLUC with the 5′ UTR of *fmr1* was due to the IRES, we measured the activity of FLUC with the 5′ UTR of *fmr1* after impairing IRES translation. RPS25 is an essential ribosomal protein that participates in the IRES-mediated translation of both *Saccharomyces cerevisiae* and mammalian, but not canonical, cap-dependent translation (42). By performing a knockdown of RPS25, we were able to create an environment where IRES-mediated translation was impaired. When we measured the activity of FLUC with the 5′ UTR of *fmr1* after the knockdown of RPS25, the activity of FLUC was significantly reduced compared to that of the control (Fig. 1B). This result may show the existence of an IRES in the 5′ UTR of *fmr1*.

To confirm the cap independence of translation in the 5′ UTR of *fmr1*, we used a monocistronic vector with an ApppG analog. The 5′ UTR of *fmr1* was inserted between the ApppG analog and the start codon of FLUC. When we measured the FLUC activity of the mRNA transcript with the 5′ UTR of *fmr1* and the ApppG analog, the activity was significantly higher than that of the mock vector (see Fig. S1B). Also, we compared the FLUC activity of ApppG capped mRNA transcript with the 5′ UTR of *fmr1* to the FLUC activity of m^7GpppG mRNA transcript with the 5′ UTR of *fmr1*, which represents total translational activity. The FLUC activity of the ApppG capped mRNA transcript with the 5′ UTR of *fmr1* maintained about 30% of the FLUC activity of the m^7GpppG capped mRNA transcript (see Fig. S1C).

In addition to IRES-mediated translation, synthesis of FLUC can be established by a cryptic promoter or ribosome reinitiation. To exclude these possibilities, we deleted the CMV promoter from one bicistronic reporter vector that contained the *fmr1* 5′ UTR (ΔCMV_5′UTR) and inserted hairpin loops upstream of RLUC into another bicistronic reporter vector (pHRF_5′UTR) (Fig. 1C). We first measured the RLUC value, which was normalized by the β-galactosidase (β-Gal) level, to see the level of cap-dependent translation. The result showed no difference between the control vector (pRF) and the vector that contained the 5′ UTR of *fmr1* (5′ UTR).The vector without a CMV promoter (ΔCMV_5′UTR) expressed no RLUC. Next, to assess IRES-mediated translation, we measured FLUC activity. A significantly higher level of FLUC activity was detected from the vector containing the *fmr1* 5′ UTR than from the control (pRF) (Fig. 1C). Moreover, the insertion of hairpin loops reduced the activities of RLUC but not the activities of FLUC, which were generated by the *fmr1* 5′ UTR. These data suggest that FLUC activities were not driven by ribosome reinitiation but by the IRES element in the 5′ UTR of *fmr1*. Although significantly reduced, FLUC activity without a CMV promoter was still detected at about 25%, suggesting the presence of a cryptic promoter in the *fmr1* 5′ UTR (Fig. 1C). We repeated this experiment with the Cos-7 cell line, which is known to contain low cryptic promoter activity (see Fig. S2A in the supplemental material) (43). Even in the Cos-7 cell line, the activity of FLUC without a CMV promoter was still detected at about 20% (see Fig. S2A). Through Northern blotting, we confirmed that expected mRNA species of 3 plasmids (5′ UTR, ΔCMV_5′UTR, and pHRF_5′UTR) were detected as a clear band with the expected size, and the mRNA of ΔCMV_5′UTR was smaller than the others, which indicated the activity of a cryptic promoter (see Fig. S2B).

FIG 1 Legend (Continued)
subjected to Western blotting, which was further analyzed using anti-RPS25 antibodies. GAPDH was used as a loading control. The table contains representative raw data that were obtained using a luminometer (MicroLumatPlus). *, $P < 0.05$; $n = 4$ independent experiments. The values represent means and SEM, and statistical significance was tested by two-way ANOVA followed by a Bonferroni *post hoc* test. (C) Dual-luciferase assays were performed using cells that were transfected with pCMV-β-gal, pRF (the backbone of the bicistronic reporter system), pRF containing the 5′ UTR of *fmr1* (5′UTR), pRF containing the 5′ UTR but lacking a CMV promoter (ΔCMV_5′UTR), and pRF containing the 5′ UTR and hairpin structure upstream of RLUC. FLUC and RLUC activities were normalized to the β-galactosidase activity. *, $P < 0.001$; $n = 5$ independent experiments. The values represent means and SEM, and statistical significance was tested by one-way ANOVA followed by a Bonferroni *post hoc* test. (D) IRES activity was measured using mRNA transcripts of reporters with deletions (Δ1-50, Δ1-65, Δ1-110, or Δ51-65) or mutations (MUT). The capped bicistronic mRNA reporters were transfected into Neuro2A cells and incubated for 6 h. With the lysate of transfected cells, firefly and renilla luciferase activities were measured using dual-luciferase assays. The table contains representative raw data that were obtained using a luminometer (MicroLumatPlus). The ratio for the reverse form of the *fmr1* 5′ UTR vector was set to 1. m^7G, 7-methyl-guanosine. **, $P < 0.01$; *, $P < 0.05$; $n = 4$ independent experiments. The values shown are means and SEM, and statistical significance was tested by one-way ANOVA followed by a Bonferroni *post hoc* test.

We also confirmed the location of this cryptic promoter by inserting serially deleted constructs of the *fmr1* 5′ UTR (Δ1-50, Δ1-65, and Δ1-110) between RLUC and FLUC in a promoterless bicistronic plasmid (see Fig. S2C).

There was significant reduction in the FLUC activity of the *fmr1* 5′ UTR with Δ1-50 and with Δ1-65, which indicated the presence of a cryptic promoter in the sequence from positions 1 to 65 (see Fig. S2C). Next, to identify the critical RNA domain for IRES activity in the 5′ UTR of *fmr1*, we aligned sequences of the *fmr1* 5′ UTR to see if there were any conserved sequences among different species (see Fig. S3A in the supplemental material). The sequence from positions 51 to 65 (^{51}TTTCGGTTTCACTTC^{65}) was pyrimidine rich and well conserved among different species, which may illustrate its importance as a critical RNA domain. To confirm the importance of the sequence, we generated deletions (Δ1-50, Δ1-65, Δ1-110, and Δ51-65) and mutations (^{51}AAAGCCAA AGTGAAG^{65}) in the conserved pyrimidine-rich domain to purine rich (Fig. 1D). We then *in vitro* transcribed these constructs, which were confirmed as homogeneous products of the expected size (see Fig. S3B). Through mRNA transfection and luciferase assay, we measured the activity of FLUC in different mRNA transcripts (Fig. 1D). The FLUC activity of the *fmr1* 5′ UTR with deletions (Δ51-65) or mutations (MUT) in the pyrimidine-rich domain was decreased significantly compared to that of the original the *fmr1* 5′ UTR. This may indicate that the conserved pyrimidine-rich sequences from positions 51 to 65 of the *fmr1* 5′ UTR are critical for the IRES activity of the *fmr1* 5′ UTR. We also checked whether the same pyrimidine sequences have any importance in the structure of the *fmr1* 5′ UTR. We predicted the structure of the *fmr1* 5′ UTR, the structure of its deleted form, and the structure of its mutated form using the mfold program (http://unafold.rna.albany.edu/?q=mfold) (see Fig. S3C). We found that the 5′ UTR of *fmr1* showed a region that contained two consecutive small loops next to a conserved pyrimidine-rich domain. When the pyrimidine-rich sequence (positions 51 to 65) was either deleted or mutated, the two small loops were lost from the structure (see Fig. S3C). This may indicate the importance of pyrimidine-rich sequences to structure, but further studies must be performed to confirm its effect on structure.

hnRNP Q binds to the *fmr1* 5′ UTR. ITAFs regulate IRES activity by controlling ribosome recruitment to the IRES element. Since our previous work showed that hnRNP Q plays a role as an ITAF for IRES-mediated translation of *AANAT*, *period1*, and *p53* (29–31), we tested if hnRNP Q also acts as an ITAF for IRES-mediated *fmr1* translation. Additionally, since polypyrimidine tract binding protein (PTB) has been proposed as a possible ITAF for IRES-mediated *fmr1* translation (38), we tested if PTB binds to the 5′ UTR of *fmr1*. To this end, we labeled the 5′ UTR RNA of *fmr1* with biotin, performed a pulldown experiment using streptavidin beads, and then tested for the presence of hnRNP Q and PTB in the pulled-down protein. As a negative control for hnRNP Q and a positive control for PTB, we used the 5′ UTR of *cry1*. A previous report showed that the 5′ UTR of *cry1* strongly binds with PTB and weakly binds with hnRNP Q (44). Figure 2A shows that hnRNP Q indeed binds to the biotinylated 5′ UTR of *fmr1*. In the case of PTB, it did not interact with the 5′ UTR of *fmr1* but only with the 5′ UTR of *cry 1*, which suggests that PTB is not an ITAF for *fmr1* translation (Fig. 2A).

Having demonstrated that hnRNP Q binds to the 5′ UTR of *fmr1*, we next tested whether the conserved pyrimidine nucleotides of *fmr1* are important for this interaction. We added the conserved pyrimidine nucleotides (^{51}UUUCGGUUUCACUUC^{65}) without biotinylation to the assay mixture (nonbiotinylated nucleotides [nt] 51 to 65). We found that the addition of nonbiotinylated nt 51 to 65 diminished the interaction between the 5′ UTR of *fmr1* and hnRNP Q in a dose-dependent manner (Fig. 2B), suggesting that the conserved pyrimidine tract likely mediates interaction between the 5′ UTR of *fmr1* and hnRNP Q. We also performed the same experiments with a mutated form of conserved pyrimidine nucleotides (^{51}AAAGCCAAAGUGAAG^{65}). The interaction between hnRNP Q and the 5′ UTR of *fmr1* did not diminish even when the level of mutated pyrimidine sequences was increased (see Fig. S4A in the supplemental material). To further verify the importance of the pyrimidine tract, we generated glutathi-

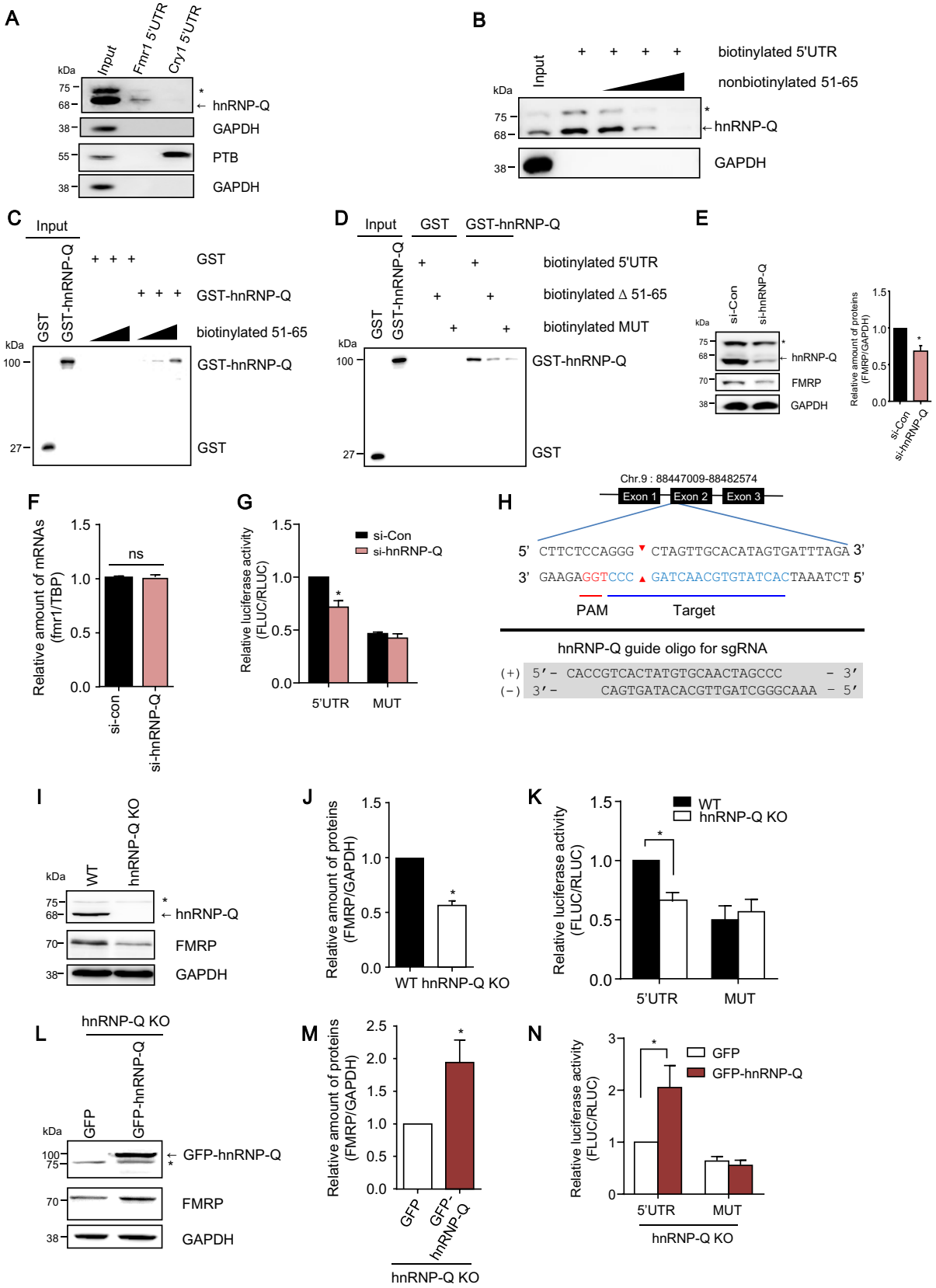

FIG 2 hnRNP Q is an ITAF required for IRES-mediated *fmr1* translation. (A to D) A streptavidin-biotin RNA affinity purification assay with Neuro2A cell extracts was used to examine if hnRNP Q binds to the biotinylated *fmr1* 5′ UTR. Biotinylated RNAs were incubated (12 h) at 4°C and pulled down using streptavidin. The pulled-down proteins were subjected to Western blotting. The asterisk indicates a nonspecific band.

(Continued on next page)

one *S*-transferase (GST)-tagged hnRNP Q (GST-hnRNP Q) and examined its ability to interact with biotinylated pyrimidine nucleotides from the 5′ UTR of *fmr1* (biotinylated nt 51 to 65). Figure 2C shows that hnRNP Q can directly interact with the pyrimidine nucleotides. Furthermore, we found that interaction between hnRNP Q and the 5′ UTR of *fmr1* was diminished when the pyrimidine-rich region was either deleted (Δ51-65) or mutated (Fig. 2D), confirming that the pyrimidine-rich region contributes to hnRNP Q binding to the 5′ UTR of *fmr1* (Fig. 2D).

hnRNP Q regulates FMRP expression. Next, we examined if hnRNP Q regulates IRES activity in the 5′ UTR of *fmr1*. First, we reduced hnRNP Q using small interfering RNA (siRNA) against *hnRNP Q* (si-*hnRNP Q*) in cells containing the bicistronic reporter system. We found that hnRNP Q and FMRP were reduced but the amount of *fmr1* transcript was not altered (Fig. 2E and F). Interestingly, knockdown of hnRNP Q significantly reduced the IRES activity of the *fmr1* 5′ UTR (Fig. 2G; see Fig. S4B), suggesting the necessity of hnRNP Q for IRES activity of the *fmr1* 5′ UTR. However, since IRES activity was not completely eliminated in these cells, either a small amount of hnRNP Q may be sufficient to activate IRES-mediated translation or other ITAFs may exist. To clarify this question, we generated the Neuro2A cell line with knockout of *hnRNP Q* using the CRISPR (clustered regularly interspaced short palindromic repeat)-Cas9 system (Fig. 2H). This cell line with an edited genome showed complete eradication of hnRNP Q and significant reduction in FMRP levels (Fig. 2I and J). Since complete deletion of hnRNP Q did not eliminate, but rather reduced, FMRP, this further suggests that *fmr1* contains a cryptic promoter and that the translation of *fmr1* may be dependent on another translation mechanism or other ITAFs. To examine the presence of other ITAFs, we measured the IRES activity of the *fmr1* 5′ UTR in *hnRNP Q* knockout cells using the bicistronic reporter system. We found that knockout of hnRNP Q reduced IRES activity in the 5′ UTR of *fmr1* (Fig. 2K; see Fig. S4C), indicating that hnRNP Q is not the only ITAF required for *fmr1* translation by the IRES mechanism. We then examined if overexpression of *hnRNP Q* restores IRES-mediated *fmr1* translation in *hnRNP Q* knockout cells (Fig. 2L). The knockout cell lines overexpressing *GFP-hnRNP Q* increased FMRP expression, as well as IRES activity, in the *fmr1* 5′ UTR (Fig. 2M and N; see Fig. S4C). In contrast, the mutated *fm1* 5′ UTR with a purine-rich domain instead of a pyrimidine-dominant region (nt 51 to 65) still showed reduced IRES activity (Fig. 2N). Together, these results confirm that hnRNP Q functions as an ITAF that is required for IRES-mediated *fmr1* translation.

FIG 2 Legend (Continued)
(A) The 5′ UTR of *cry1* was used as a negative control for hnRNP Q and as a positive control for PTB. (B) Biotinylated *fmr1* 5′ UTR was incubated (12 h) at 4°C with cell lysates in the presence of 15 nonbiotinylated pyrimidine-rich nucleotides (^{51}UUUCGGUUUCACUUC^{65}) with different concentrations (5 μM, 10 μM, and 15 μM) and pulled down with streptavidin. (C) Different amounts of 15 biotinylated pyrimidine-rich nucleotides (5 μM, 10 μM, and 15 μM) were incubated (12 h) at 4°C with GST or GST-hnRNP Q. (D) Either biotinylated *fmr1* 5′ UTR, biotinylated *fmr1* 5′ UTR with deletions (Δ51-65), or biotinylated *fmr1* 5′ UTR with mutations (Fig. 1D) was incubated (12 h) at 4°C with GST or GST-hnRNP Q. (E) Neuro2A cells were transfected with either si-Con or si-hnRNP Q. The cell lysates were subjected to Western blotting, which was further analyzed. GAPDH was used as a loading control. The level of FMRP was normalized to that of GAPDH. *, $P < 0.05$; $n = 5$ independent experiments. The values shown are means and SEM, and statistical significance was tested by *t* test. (F) Real-time quantitative PCR was performed with cell lysates shown in panel E. The level of *fmr1* mRNA transcript was normalized to that of TBP mRNA transcript. $n = 3$ independent experiments. The values shown are means and SEM, and statistical significance was tested by *t* test. ns, not significant. (G) A dual-luciferase assay was performed with Neuro2A cells that were transfected with either pRF *fmr1* 5′ UTR or pRF *fmr1* 5′ UTR with mutations (24 h) after si-Con or si-hnRNP Q transfection (24 h). The activity of FLUC was normalized by the activity of RLUC. *, $P < 0.05$; $n = 5$ independent experiments. The values shown are means and SEM, and statistical significance was measured by two-way ANOVA followed by a Bonferroni *post hoc* test. (H) CRISPR/Cas9 was used to knock out the *hnRNP Q* locus on mouse chromosome 9. Arrowheads show the expected cleavage sites. (I) Cell lysates from the wild-type Neuro2A cell line and the hnRNP Q KO cell line were subjected to Western blotting. GAPDH was used as a loading control. (J) Quantification data from panel I. *, $P < 0.005$; $n = 3$ independent experiments. The values shown are means and SEM, and statistical significance was tested by *t* test. (K) A dual-luciferase assay was performed with both the Neuro2A cell line and the hnRNP Q KO cell line, which were transfected with either pRF *fmr1* 5′ UTR or pRF *fmr1* 5′ UTR with mutations (24 h). The activity of FLUC was normalized by the activity of RLUC. *, $P < 0.01$; $n = 3$ independent experiments. The values shown are means and SEM, and statistical significance was tested by two-way ANOVA followed by a Bonferroni *post hoc* test. (L) hnRNP Q KO cells were transfected with either GFP or GFP-hnRNP Q vector. The cell lysates were subjected to Western blotting. GAPDH was used as a loading control. (M) Quantification data from panel L. *, $P < 0.05$; $n = 4$ independent experiments. The values shown are means and SEM, and statistical significance was tested by *t* test. (N) A dual-luciferase assay was performed with hnRNP Q KO cells that were transfected with either pRF *fmr1* 5′ UTR or pRF *fmr1* 5′ UTR with mutations (24 h) after GFP or GFP-hnRNP Q transfection (24 h). The activity of FLUC was normalized by the activity of RLUC. *, $P < 0.05$; $n = 4$ independent experiments. The values shown are means and SEM, and statistical significance was tested by two-way ANOVA followed by a Bonferroni *post hoc* test.

FMRP expression uses both cap-dependent and cap-independent translation. We demonstrated that FMRP expression utilizes IRES-mediated translation, but there was still a possibility that FMRP uses a cap-dependent expression mechanism (Fig. 2J). Moreover, conflicting results were reported regarding the mechanism of *fmr1* translation (39, 40). Thus, to investigate if FMRP expression also uses cap-dependent translation, we treated Neuro2A cells with an inhibitor of mTOR, RAD001. 4E-BP represses mRNA translation, but phosphorylation of 4E-BP by mTOR dissociates 4E-BP from the cap-binding complex to enable mRNA translation to occur (45). Thus, RAD001 treatment prevents canonical cap-dependent translation through inhibition of mTOR, which blocks phosphorylation of 4E-BPs (46). Neuro2A cells incubated with RAD001 showed no change in FMRP expression, but there was a reduction in phosphorylation of 4E-BP (Fig. 3A and B). Cycloheximide (CHX), which blocks translation elongation, reduced FMRP but not phospho-4E-BP (Fig. 3A and B), since phospho-4E-BP is more stable than FMRP during the period of CHX treatment. GAPDH (glyceraldehyde-3-phosphate dehydrogenase) was used as a loading control, because it has a long half-life. We also reduced eukaryotic initiation factor 4E (eIF-4E) by using siRNA. The cells containing *eIF-4E* siRNAs showed a decrease in p21 levels, which are known to depend on eIF-4E-dependent translation, but the FMRP level was not altered (Fig. 3C and D). Together, these results support the idea that the 5′ UTR of *fmr1* has an IRES mechanism, consistent with the results shown in Fig. 1 and 2. However, *eIF-4E* siRNAs might not have been fully effective in blocking cap-dependent translation, since a significant amount of p21 was still expressed. To further confirm that *fmr1* indeed uses both cap-dependent and cap-independent translation, we then treated *hnRNP Q* knockout cells with RAD001. *hnRNP Q* knockout cells treated with dimethyl sulfoxide (DMSO) showed almost 50% reduction of the FMRP level, consistent with the result shown in Fig. 2J. However, RAD001 treatment further decreased the FMRP level, suggesting that FMRP expression is regulated by cap-dependent translation, as well (Fig. 3E and F). The expression level of p21 showed no difference in DMSO-treated cells, while it showed a reduction in RAD001-treated cells (Fig. 3E and F).

Sema3A upregulates hnRNP Q, followed by IRES-mediated *fmr1* translation. Next, we set out to understand the physiological significance of hnRNP Q- and IRES-mediated *fmr1* translation. Knockout of *fmr1* in primary hippocampal neurons had been shown to diminish Sema3A-induced axonal growth cone collapse (36), but the underlying mechanism was still incompletely understood. We proposed that Sema3A (250 ng/ml; 30 min)-induced growth cone collapse was due to upregulation of hnRNP Q, followed by IRES-mediated *fmr1* translation in neurons (34). To test this hypothesis, we first examined whether Sema3A treatment increases hnRNP Q synthesis in primary hippocampal neurons. To this end, we used a fluorescent noncanonical amino acid-tagging proximity ligation assay (FUNCAT-PLA) that enables visualization of newly synthesized protein *in situ*. After treating neurons with Sema3A, newly synthesized hnRNP Qs were detected by proximity ligation following coincident detection of hnRNP Q antibody and biotin antibody in neurons that had taken up azidohomoalanine (AHA) (Fig. 4A). AHA is an amino acid analog of methionine that can be labeled by biotin. No newly synthesized hnRNP Q protein was detected in the control neurons containing methionine instead of AHA or in neurons treated with anisomycin, a translation inhibitor (Fig. 4A). These results show upregulation of the hnRNP Q level in hippocampal primary neurons by Sema3A treatment. We then used the same method to detect newly synthesized FMRP in neurons treated with Sema3A. FMRPs were clearly seen in the primary neurons compared to the control and anisomycin-treated neurons (Fig. 4B). Together, these results indicated that Sema3A treatment indeed increases expression of hnRNP Q and FMRP in hippocampal primary neurons. We next examined whether IRES-mediated *fmr1* translation was responsible for the newly synthesized FMRP after Sema3A treatment. To this end, we generated a modified bicistronic reporter system that replaced RLUC and FLUC with mCherry and Flag, respectively. Then, the 5′ UTR of *fmr1* was inserted in front of Flag. Using FUNCAT-PLA, we detected the newly synthesized Flag peptide only after treating neurons with Sema3A. The control and

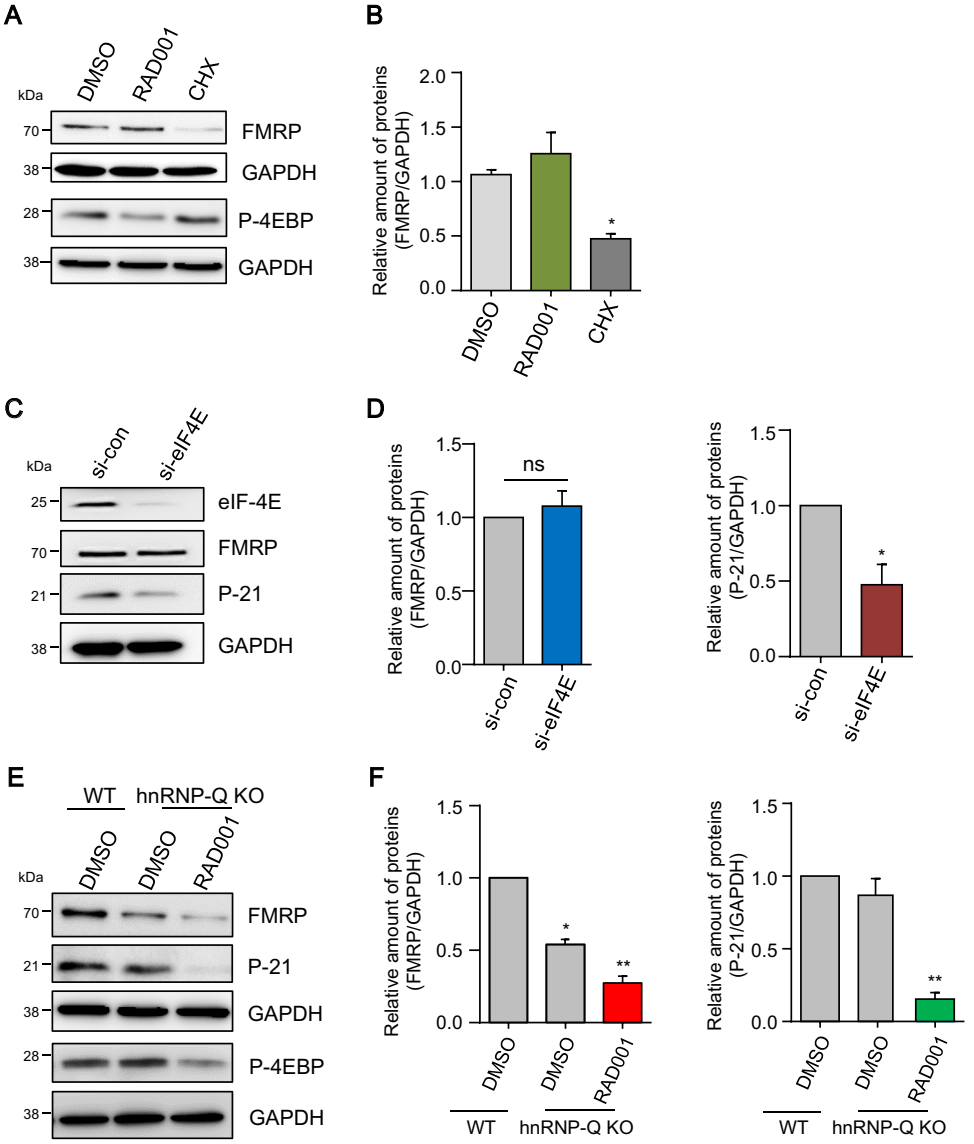

FIG 3 FMRP expression is significantly reduced in hnRNP Q knockout cells treated with RAD001. (A) Neuro2A cells were treated with either dimethyl sulfoxide (DMSO), RAD001, or cycloheximide and incubated for 24 h. The lysates from the cells were then subjected to Western blotting. GAPDH was used as a loading control. (B) Quantification data from panel A produced with Prism from GraphPad. The protein level of FMRP was normalized by GAPDH. *, $P < 0.001$; $n = 4$. The values shown are means and SEM and were tested for statistical significance by one-way ANOVA followed by a Bonferroni *post hoc* test. (C) Neuro2A cells were transfected with either si-Con or si-eIF-4E for 48 h. The lysates from the cells were used for Western blotting. GAPDH was used as a control. (D) Quantification data from panel C obtained with Prism from GraphPad. The protein levels of FMRP and p-21 were normalized by GAPDH. *, $P < 0.05$; ns, not significant; $n = 4$. The values shown are means and SEM and were tested for statistical significance by *t* test. (E) Wild-type Neuro2A and hnRNP Q KO cell lines were treated with either DMSO or RAD001 for 24 h. The cells were harvested, and the lysates were subjected to Western blotting. GAPDH was used as a loading control. (F) Quantification data from panel E obtained with Prism from GraphPad. The protein levels of FMRP and p-21 were normalized by GAPDH. *, $P < 0.05$; **, $P < 0.001$; $n = 4$. The values shown are means and SEM and were tested for statistical significance by one-way ANOVA followed by a Bonferroni *post hoc* test.

anisomycin-treated cells generated no newly synthesized Flag (Fig. 4C). When we substituted the 5′ UTR of *fmr1* for the 5′ UTR of *fmr1* with deletions (Δ51-65), no newly synthesized Flag peptide was observed, even after treatment with Sema3A (see Fig. S5A in the supplemental material). Together, these results indeed suggest that Sema3A triggers IRES-mediated *fmr1* translation in primary hippocampal neurons.

To further verify that Sema3A induces IRES activity in the *fmr1* 5′ UTR, we transfected a bicistronic reporter with RLUC/FLUC into Neuro2A cells and measured IRES

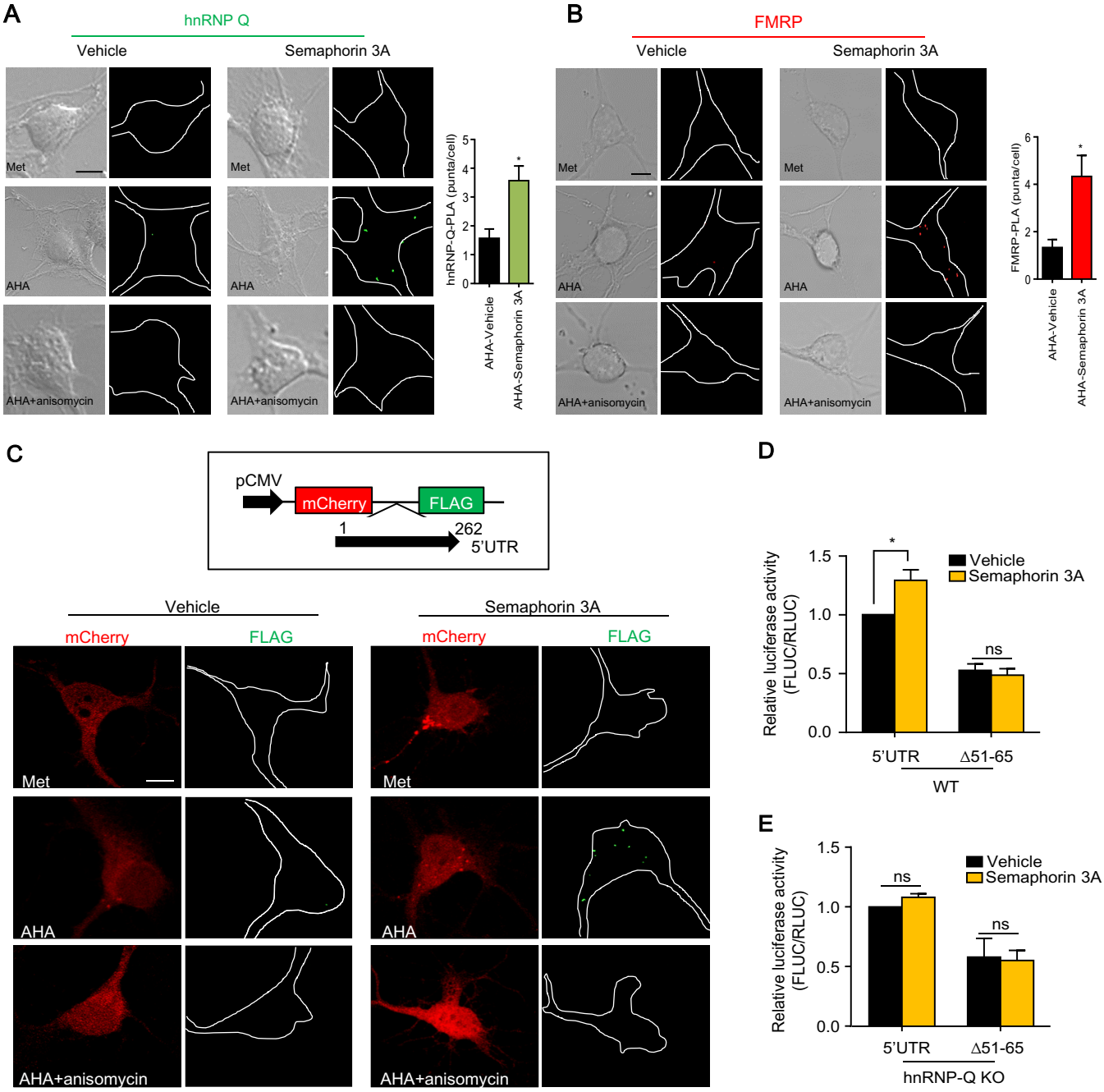

FIG 4 Sema3A triggers new synthesis of hnRNP Q and FMRP in hippocampal primary neurons. (A) (Left) Newly synthesized hnRNP Q was detected using the FUNCAT-PLA method. Hippocampal primary neurons treated with Sema3A (250 ng/ml; 30 min) were incubated with AHA, an amino acid analog of methionine that enables labeling by biotin. Newly synthesized hnRNP Qs were detected by proximity ligation following coincident detection of hnRNP Q antibody and biotin antibody. New synthesis of hnRNP Q in neurons was blocked with anisomycin (40 μM). Scale bar = 10 μm. (Right) Quantification of hnRNP Q FUNCAT-PLA signals with Sema3A normalized to vehicle in AHA labeling. $n = 18$ to 20 cells per condition from three different experiments. *, $P < 0.01$. The values shown are means and SEM and were tested for statistical significance by *t* test. (B) (Left) The same method was applied to detect newly synthesized FMRP after Sema3A treatment. New FMRP was clearly found in neurons treated with Sema3A (250 ng/ml; 30 min). Scale bar = 10 μm. (Right) Analysis of FMRP FUNCAT-PLA signals with Sema3A normalized to vehicle in AHA labeling. $n = 18$ to 20 cells per condition from three different experiments. *, $P < 0.05$. The values shown are means and SEM and were tested for statistical significance by *t* test. (C) A modified bicistronic reporter in which RLUC and FLUC were replaced with mCherry and Flag, as well as having the 5′ UTR of *fmr1* in front of Flag, was transfected into primary neurons. After Sema3A treatment (250 ng/ml; 30 min) as for panels A and B, FUNCAT-PLA was applied to detect newly synthesized Flag peptide. Scale bar = 5 μm. (D and E) The bicistronic reporter containing the 5′ UTR of *fmr1* or the 5′ UTR of *fmr1* with deletions (Δ51-65) was transfected into the Neuro2A cell line (D) or the hnRNP Q KO cell line (E). A dual-luciferase assay was performed after Sema3A treatment (250 ng/ml; 1 h). The data were measured and analyzed by the same method as for Fig. 1A. *, $P < 0.05$; ns, not significant; $n = 3$ independent experiments. The values shown are means and SEM and were tested for statistical significance by two-way ANOVA followed by a Bonferroni *post hoc* test.

activity (47). Indeed, Sema3A treatment significantly increased IRES activity compared to that of the control, while the 5′ UTR of *fmr1* with deletions (Δ51-65) showed no difference (Fig. 4D; see Fig. S5B). Also, to examine whether hnRNP Q takes part in the induction of IRES activity by Sema3A treatment, we repeated the same experiment with the *hnRNP Q* KO cell line (Fig. 4E; see Fig. S5C). The increase of IRES activity by Sema3A treatment seen in the Neuro2A cell line was not observable in the *hnRNP Q* KO cell line. While the mechanism behind this process remains unknown, this may indicate the importance of hnRNP Q in the induction of IRES activity of *fmr1* by Sema3A.

hnRNP Q is important in Sema3A-induced axonal growth cone collapse. We showed that Sema3A triggered new synthesis of hnRNP Q and FMRP in hippocampal primary neurons (Fig. 4A and B). Furthermore, IRES-mediated *fmr1* translation in primary neurons was activated by Sema3A treatment (Fig. 4C). Next, we wanted to further investigate if Sema3A-induced axonal growth cone collapse is due to IRES-mediated *fmr1* translation. To this end, we first examined if *hnRNP Q* or *fmr1* overexpression causes growth cone collapse. We found that primary neurons containing high levels of hnRNP Q or FMRP produced growth cone collapse (Fig. 5A to D). Next, we tested if *fmr1* siRNA transfection into neurons rescues Sema3A-induced axonal growth cone collapse. The knockdown of *fmr1* was confirmed through measurement of the intensity of the FMRP signal (see Fig. S5D). As expected, transfecting *fmr1* siRNA into neurons prevented axonal growth cone collapse when the neurons were treated with Sema3A (Fig. 5E and F), which is consistent with reports showing that Sema3A-induced growth cone collapse is diminished in *fmr1* knockout primary neurons (36). Since we showed that hnRNP Q is an ITAF for IRES-mediated *fmr1* translation, we then asked if Sema3A-induced growth cone collapse is attenuated by reducing hnRNP Q. In contrast to control neurons with collapsed growth cones after Sema3A treatment, the amount of axonal growth cone collapse in *hnRNP Q* siRNA-transfected neurons was significantly attenuated (Fig. 5G and H). The knockdown of *hnRNP Q* was also confirmed through measurement of the intensity of the hnRNP Q signal (see Fig. S5E). Together, these results demonstrate that Sema3A-induced growth cone collapse is due to upregulation of hnRNP Q, followed by IRES-mediated *fmr1* translation.

DISCUSSION

As loss of FMRP causes FXS, the functions of the FMRP protein in neurons and the transcriptional regulation of *fmr1* have been intensively studied. However, the mechanisms regulating *fmr1* translation are poorly understood. Two studies showed that *fmr1* utilizes IRES-mediated translation, while Ludwig et al. claimed that *fmr1* uses only a canonical cap-dependent translation mechanism (38–40). Ludwig et al. used hairpin-forming nucleotides shown to prevent initiation of cap-dependent translation for their study (14, 48). These nucleotides were introduced near the tip of the 5′ UTR of *fmr1*, and *fmr1* translation was completely blocked. It was thus concluded that FMRP synthesis utilizes mostly cap-dependent translation. However, it is plausible that the hairpin-forming nucleotides inserted into the 5′ UTR of *fmr1* might also interfere with ribosome recruitment for cap-independent translation. Here, we discovered that hnRNP Q is an ITAF for IRES-mediated *fmr1* translation. When the cap-dependent translation mechanism was inhibited by RAD001 or *eIF-4E* siRNA, FMRP expression was not altered (Fig. 3A to D). However, if IRES-mediated *fmr1* translation was prevented through deletion of ITAF, FMRP expression dropped (Fig. 2I and J). When both cap-dependent and IRES-mediated translations were inhibited at the same time, FMRP was further decreased (Fig. 3E and F). Altogether, it is plausible that *fmr1* indeed uses both cap-dependent and cap-independent translation.

Li et al. discussed Sema3A-induced axonal growth cone reduction in *fmr1* knockout hippocampal primary neurons, since Sema3A failed to increase eIF-4E phosphorylation (36). They also showed that *fmr1* knockout neurons attenuated Sema3A-induced axonal growth cone collapse. However, our results suggest that Sema3A-induced growth cone collapse is mostly due to upregulation of hnRNP Q followed by FMRP increase. Cap-dependent *fmr1* translation through eIF-4E phosphorylation makes a minimal

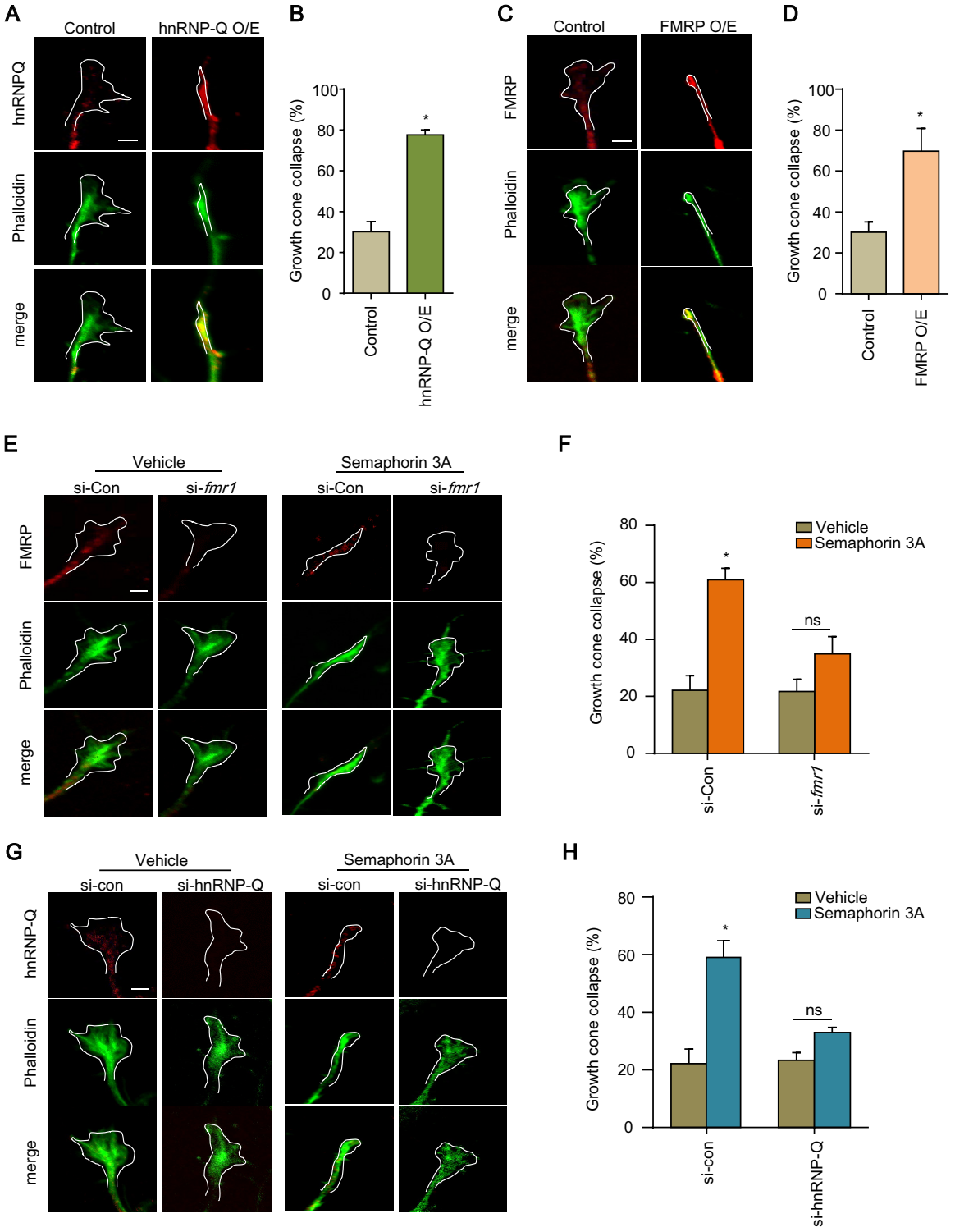

FIG 5 Sema3A-induced axonal growth cone collapse is due to hnRNP Q expression. (A and B) Hippocampal primary neurons were transfected with hnRNP Q overexpression (O/E) vector with mCherry at DIV1. Axonal growth cones collapse was detected with phalloidin antibody at DIV3. Immunocytochemistry was performed with phalloidin antibody after the fixation of primary neurons. The images were taken with an LSM780 confocal microscope. *, $P < 0.0001$; $n = 47$ (total number of axonal growth cones examined) from 3 independent experiments. The values shown are means and SEM and were tested for statistical significance by *t* test. (C and D) Primary neurons were transfected with FMRP overexpression vector with mCherry at DIV1. Axonal growth cone collapse was detected with phalloidin antibody at DIV3. *, $P < 0.01$; $n = 50$ (total number of axonal growth cones examined) from 3 independent experiments. The values shown are means and SEM and were tested for statistical significance by *t* test. (E and F) Primary neurons were treated with Sema3A (250 ng/ml; 30 min) at DIV3 after the transfection of either si-Con or si-*fmr1* at DIV1. Immunocytochemistry was performed with FMRP antibody after the fixation of primary neurons. *, $P < 0.05$; $n = 86$ (total number of axonal growth cones examined) from 3 independent experiments.

(Continued on next page)

contribution, since *hnRNP Q* reduction fully prevented growth cone collapse caused by Sema3A treatment. Also, blocking cap-dependent translation of *fmr1* with RAD001 or reduction of *eIF-4E* alone did not alter FMRP expression, while reducing *hnRNP Q* evidently decreased the amount of FMRP. Together, our results imply that IRES-mediated *fmr1* translation activated by hnRNP Q is responsible for Sema3A-induced axonal growth cone collapse.

In summary, we demonstrated that *fmr1* translation utilizes both cap-dependent and IRES-mediated mechanisms. Furthermore, we found that hnRNP Q acts as an ITAF for IRES-mediated *fmr1* translation and that Sema3A induces new synthesis of hnRNP Q and FMRP in hippocampal primary neurons. Finally, we showed that upregulation of hnRNP Q, followed by FMRP synthesis, is the cause of Sema3A-induced axonal growth cone collapse. As lack of FMRP generates fragile X syndrome and autism, our work on the regulatory mechanism of FMRP synthesis may provide new insights into the molecular and cellular mechanisms underlying such disorders.

MATERIALS AND METHODS

Animal care. Animals were used in accordance with protocols approved by the Animal Care and Use Committees of Pohang University of Science and Technology and Ulsan National Institute of Science and Technology. The C57BL/6 mouse strain was purchased from Hyochang Science.

Cell culture. Dulbecco's modified Eagle's medium (DMEM) (HyClone) with 10% fetal bovine serum (FBS) (HyClone) and 1% penicillin-streptomycin (Welgene) was used to culture Neuro2A cells. For transfection, Lipofectamine 2000 (Invitrogen) was used. Primary hippocampal neurons were dissected from embryonic day 18 (E18) mouse embryos. Either 12-mm glass coverslips or 35-mm glass bottom dishes (WillCo Wells) coated with poly-D-lysine (50 μg/ml; Sigma) were used to seed the neurons. Neuro2A cells were treated with 20 nM RAD001 (159351-69-6; InvivoGen) or 100 μg/ml cycloheximide and then harvested at the indicated times.

Plasmid construction. The 5′ UTR of mouse *fmr1* (NM_008031.2) (https://www.ncbi.nlm.nih.gov/nuccore/NM_008031.2/) (AGGAGGCGCAGCGGAGCCCTTGGCCTCAGTCAGTCAGGCGCTGGGGAGCGTTTCG GTTTCACTTCCGGTGAGGGGCCGCGCCTGAGAGGGCGGGCAGTGAAGCAAACGGACGGCGAGCGCGGGCGGT GGCAGTGACGGCGGCGCCGCTGCCGGGGGGCGTGCGGTAACGCGGCGGCGGCGGCGGCGGCGACGGCGGCT GGGCCTCAAGCGCCTGCAGCCCACCTCCCGGAGGCGGGCTCCCGGCGCGAGGACGGACGAGAAG) was amplified from cDNA using *PFU* polymerase (Solgent) and was confirmed by sequencing. All the PCR products were digested with SalI/XmaI restriction enzymes (Beams) and inserted into the intercistronic region of a pRF bicistronic vector that contained both RLUC and FLUC (19, 20, 24, 30). For the pRF bicistronic vector with the promoter deleted (ΔCMV_5′UTR), the CMV promoter was removed from the pRF bicistronic vector by digestion with BglIII/NheI restriction enzymes and self-ligation. For the binding assay, fragments of the *fmr1* 5′ UTR were digested and subcloned into the pBluescript SK vector. To generate the bicistronic mRNA transcripts, fragments of the *fmr1* 5′ UTR were inserted into the SalI/BamHI site of pCY2-RF. The following primers were used: 5′ UTR, forward, AAGAATTCAGGAGGCGCAGCGGAGC, and reverse, GGGC TTCTCGTCCGTCCTCGCGCC; Δ1-50, forward, AAGAATTCTTTCGGTTTCACTTCCGGT, and reverse, GGGCTTC TCGTCCGTCCTCGCGCC; Δ1-65, forward, AAGAATTCCGGTGAGGGGCCGCGCCT, and reverse, GGGCTTCTC GTCCGTCCTCGCGCC; Δ1-110, forward, AAGAATTCCGGCGAGCGCGGGCGGTG, and reverse, GGGCTTCTC GTCCGTCCTCGCGCC.

RNA interference (RNAi) transfection. For siRNA transfection into Neuro2A cells, a microporator (Digital-Bio, Seoul, Republic of Korea) was used according to the manufacturer's instructions with the following conditions: 1,100 V, 30 ms, and 2 pulses. After 24 h of incubation, cells were harvested for further experiments. The siRNAs that we used in our experiments are as follows: si-RPS 25 (Ambion 16708; 5′-GUAAAUAAAUCUGGUGGCATT-3′), si-eIF-4E (Cell Signaling; 6424), si-FMRP (Santa Cruz; sc-36871), and si-*hnRNP Q* (Santa Cruz; sc-72097).

mRNA transfection. A bicistronic vector was initially linearized with EcoRI, and then, the reporter mRNAs were synthesized by *in vitro* transcription with SP6 polymerase (Roche) in the presence of m^7G(5′)ppp(5′), a cap analog (Roche). *In vitro*-transcribed mRNA was purified by phenol-chloroform extraction and 3 M sodium acetate precipitation. Neuro2A cells were transiently transfected with 2 μg of the capped reporter mRNAs for 6 h using Lipofectamine 2000 (Invitrogen).

Luciferase assay. Cells were harvested and resuspended in luciferase lysis buffer (Promega) and then incubated on ice for 10 min. Cell debris was removed by centrifugation at 15,000 rpm at 4°C for 10 min. The supernatants were used for the luciferase assay. According to the manufacturer's instructions, a

FIG 5 Legend (Continued)
The values shown are means and SEM and were tested for statistical significance by two-way ANOVA followed by a Bonferroni *post hoc* test. (G and H) Primary neurons were treated with Sema3A (250 ng/ml; 30 min) at DIV3 after the transfection of either si-Con or si-hnRNP Q at DIV1. Immunocytochemistry was performed with hnRNP Q antibody after the fixation of primary neurons. *, $P < 0.01$; $n = 60$ (total number of axonal growth cones examined) from 3 independent experiments. The values shown are means and SEM and were tested for statistical significance by two-way ANOVA followed by a Bonferroni *post hoc* test.

Dual-Luciferase reporter assay system (Promega) was used to measure firefly and renilla luciferase activities. IRES activity was represented by the ratio of firefly luciferase activity to renilla luciferase activity.

β-Galactosidase assay. Cells were transfected with the β-galactosidase expression vector. After harvesting, these cells were resuspended in luciferase lysis buffer (Promega) and incubated on ice for 10 min. Reagents (phosphate-buffered saline [PBS] containing 5 mM EDTA, chlorophenol red–β-D-galactopyranoside [CPRG], and β-Gal buffer) were used to incubate cell lysates at room temperature (RT). After confirming the endpoint, β-galactosidase activities were measured with a plate reader at a wavelength of 570 nm.

Quantitative real-time PCR. Quantitative real-time PCR (qPCR) was performed as previously described (49). After the isolation of total RNAs using TRI reagent (Molecular Research Center), 1 μg of total RNA was used for cDNA synthesis with oligo(dT). Reverse transcription was performed using the ImProm-II reverse transcription system (Promega). Then, the expression levels of mRNA transcripts were analyzed by quantitative real-time PCR using a StepOnePlus real-time PCR system (Applied Biosystems) with SYBR green master mix (Roche). qPCR was performed with an initial denaturation step at 95°C for 10 min, followed by 45 cycles of denaturation at 95°C for 15 s and annealing at 60°C for 30 s. All samples were tested in triplicate. The primer sequences were as follows: *fluc*, forward, GAGGTTCCATCTGCCAG GTA, and reverse, CACACAGTTCGCCTCTTTGA; *rluc*, forward, AACGCGGCCTCTTCTTATTT, and reverse, ACCAGATTTGCCTGATTTGC; *mfmr1*, forward, TTGAAAACAACTGGCAACCA, and reverse, CACCAACAGCAA GGCTCTTT; *mTBP*, forward, CAGCCTTCCACCTTATGCTC, and reverse, TTGCTGCTGTCTTTGTT; *mgapdh*, forward, GTCTTCCTGGGCAAGCAGTA, and reverse, CTGGACAGAAACCCCACTTC.

Northern blotting. For Northern blotting, RNA was extracted from Neuro2A cells using TRI-Reagent (Molecular Research Center, Cincinnati, OH). The total RNA (5 μg) was size separated by 1% formaldehyde-agarose gel electrophoresis with 0.66 M formaldehyde, transferred to nylon membranes (Pall Corporation, Port Washington, NY), and hybridized with a randomly primed probe labeled with [^{32}P]dCTP (PerkinElmer). For detection of reporter mRNA, the *fluc* coding region was used as a probe. Radioactivity was analyzed by autoradiography.

CRISPR-Cas9 method. The pSpCas9(BB)-2A-Puro (PX459) plasmid from Addgene (catalog no. 62988) was used to create the single guide RNA (sgRNA) expression construct. Design and preparation of sgRNAs were done as previously described (50), and an online CRISPR design tool (http://crispr.mit.edu) was used to investigate the off-target effects of sgRNA candidates. The target double-stranded DNA (dsDNA) was generated by annealing two oligonucleotides (top, CACCGTCACTATGTGCAACTAGCCC, and bottom, CAGTGATACACGTTGATCGGGCAAA) and was later cloned into PX459 vectors.

Western blotting. Immunoblot analysis was performed with the following primary antibodies: polyclonal anti-FMRP (Cell Signaling; 4317; 1:1,000), monoclonal anti-phospho-rpS6 (Cell Signaling; 9206; 1:1,000), monoclonal anti-eIF-4E (Abcam; 171091; 1:500), and monoclonal anti-hnRNP Q (Abcam; 1:1,000). Enhanced chemiluminescence (ECL) solution and a LAS-4000 chemiluminescence detection system were used to visualize horseradish peroxidase (HRP)-conjugated secondary antibodies.

Immunocytochemistry. Hippocampal primary neurons were fixed in prewarmed 4% paraformaldehyde (PFA) for 15 min at RT. Then, the neurons were washed with PBS twice for 10 min each time. After the neurons were permeabilized with 0.5% Triton X-100 containing PBS for 15 min at RT, they were blocked for 1 h at RT with 1% bovine serum albumin (BSA) containing PBS. Immunostaining was carried out with hnRNP Q antibody (Abcam; 1:100) overnight at 4°C. Then, Alexa Fluor-conjugated antibody (Invitrogen; 1:2,000) was used as the secondary antibody for 1 h at RT. Images were taken with an LSM780 confocal microscope (Zeiss).

FUNCAT-PLA. FUNCAT-PLA was performed as previously described (51). Plasmids were transfected into hippocampal primary neurons of mice at day 1 *in vitro* (DIV1). Neurons at DIV2 were cultured in Met-free DMEM (Gibco; catalog no. 21013-024) for 30 min, followed by addition of 4 mM AHA (Invitrogen; catalog no. C10102), and for 1 h to carry out metabolic labeling. As a negative control, 4 mM methionine (Sigma; M0960000) was used instead of AHA. The neurons were fixed with 4% PFA-sucrose for 20 min and permeabilized with 0.5% Triton X-100. Next, a click reaction was performed by adding chemicals, such as 200 mM Tris(1-benzyl-4-triazolylmethyl)amine (TBTA) (Sigma; catalog no. 678937), 500 mM Tris(2-carboxyethyl)phosphine hydrochloride (TCEP) (Sigma; catalog no. 646547), 25 mM biotin-alkyne (Jena Bioscience; catalog no. CLK-TA105-25), and 200 mM $CuSO_4$ (Sigma; catalog no. C1297) after blocking the neurons with 4% goat serum (Gibco; catalog no. PCN5000). Then, Duolink reagents (Sigma; Duo92013) were used to perform a PLA according to the manufacturer's instructions. For primary antibodies, biotin antibody (1:1,500; Sigma; catalog no. B7653) and Flag antibody (1:1,500; Sigma; catalog no. F7425) were used.

Streptavidin-biotin RNA affinity purification assay. The *fmr1* 5′ UTR was synthesized by *in vitro* transcription with T7 RNA polymerase (Roche) in the presence of biotinylated UTP. Then, cytoplasmic extracts from Neuro2A cells in dialysis buffer (10 mM HEPES, 90 mM potassium acetate [KOAc], 1.5 mM magnesium acetate [MgOAc], 2.5 mM dithiothreitol [DTT]) were used to incubate the biotin-labeled *fmr1* 5′ UTR. To perform the competition experiment, 10× unlabeled *fmr1* 5′ UTR was added to the reaction buffer containing the biotin-labeled *fmr1* 5′ UTR and incubated for 30 min. Then, streptavidin-agarose resin (Thermo Scientific; catalog no. 20349) was added and further incubated for 12 h at 4°C in a rotary mixer. After the resins were washed three times with dialysis buffer (1% NP40), resin-bound proteins were eluted and used for immunoblotting.

Statistical analysis. Statistical significance was performed by Student's *t* test, one-way analysis of variance (ANOVA), and two-way ANOVA, followed by a Bonferroni *post hoc* test using Prism 5.0 software (GraphPad).

SUPPLEMENTAL MATERIAL

Supplemental material for this article may be found at https://doi.org/10.1128/MCB.00371-18.

SUPPLEMENTAL FILE 1, PDF file, 4.4 MB.

ACKNOWLEDGMENTS

This work was supported by the Bio & Medical Technology Development Program of the National Research Foundation (NRF) funded by the Korean government (MSIT) (2018011982), the Basic Research Program (18-BR-03) funded by the Korea Brain Research Institute (KBRI), the Cooperative Research Program for Agriculture Science and Technology Development (project no. PJ01324801) of the Rural Development Administration, and also by BK21 Plus (10Z20130012243) funded by the Ministry of Education, Republic of Korea. The work was also partly supported by the Leading Research Program (2016R1A3B1905982 to K.-T.M.) of the NRF.

REFERENCES

1. Bagni C, Oostra BA. 2013. Fragile X syndrome: from protein function to therapy. Am J Med Genet A 161A:2809–2821. https://doi.org/10.1002/ajmg.a.36241.
2. Bassell GJ, Warren ST. 2008. Fragile X syndrome: loss of local mRNA regulation alters synaptic development and function. Neuron 60:201–214. https://doi.org/10.1016/j.neuron.2008.10.004.
3. Sethna F, Moon C, Wang H. 2014. From FMRP function to potential therapies for fragile X syndrome. Neurochem Res 39:1016–1031. https://doi.org/10.1007/s11064-013-1229-3.
4. Todd PK, Oh SY, Krans A, He F, Sellier C, Frazer M, Renoux AJ, Chen KC, Scaglione KM, Basrur V. 2013. CGG repeat-associated translation mediates neurodegeneration in fragile X tremor ataxia syndrome. Neuron 78:440–455. https://doi.org/10.1016/j.neuron.2013.03.026.
5. Usdin K, Woodford KJ. 1995. CGG repeats associated with DNA instability and chromosome fragility form structures that block DNA synthesis in vitro. Nucleic Acids Res 23:4202–4209.
6. Willemsen R, Levenga J, Oostra BA. 2011. CGG repeat in the FMR1 gene: size matters. Clin Genet 80:214–225. https://doi.org/10.1111/j.1399-0004.2011.01723.x.
7. Antar LN, Dictenberg JB, Plociniak M, Afroz R, Bassell GJ. 2005. Localization of FMRP-associated mRNA granules and requirement of microtubules for activity-dependent trafficking in hippocampal neurons. Genes Brain Behav 4:350–359. https://doi.org/10.1111/j.1601-183X.2005.00128.x.
8. Price TJ, Flores CM, Cervero F, Hargreaves KM. 2006. The RNA binding and transport proteins staufen and fragile X mental retardation protein are expressed by rat primary afferent neurons and localize to peripheral and central axons. Neuroscience 141:2107–2116. https://doi.org/10.1016/j.neuroscience.2006.05.047.
9. Schaeffer C, Beaulande M, Ehresmann C, Ehresmann B, Moine H. 2003. The RNA binding protein FMRP: new connections and missing links. Biol Cell 95:221–228. https://doi.org/10.1016/S0248-4900(03)00037-6.
10. Wang W, Zhu JZ, Chang KT, Min KT. 2012. DSCR1 interacts with FMRP and is required for spine morphogenesis and local protein synthesis. EMBO J 31:3655–3666. https://doi.org/10.1038/emboj.2012.190.
11. Pfeiffer BE, Huber KM. 2007. Fragile X mental retardation protein induces synapse loss through acute postsynaptic translational regulation. J Neurosci 27:3120–3130. https://doi.org/10.1523/JNEUROSCI.0054-07.2007.
12. Weiler IJ, Irwin SA, Klintsova AY, Spencer CM, Brazelton AD, Miyashiro K, Comery TA, Patel B, Eberwine J, Greenough WT. 1997. Fragile X mental retardation protein is translated near synapses in response to neurotransmitter activation. Proc Natl Acad Sci U S A 94:5395–5400.
13. Zhang J, Roberts R, Rakotondrafara AM. 2015. The role of the 5′ untranslated regions of Potyviridae in translation. Virus Res 206:74–81. https://doi.org/10.1016/j.virusres.2015.02.005.
14. Babendure JR, Babendure JL, Ding J-H, Tsien RY. 2006. Control of mammalian translation by mRNA structure near caps. RNA 12:851–861. https://doi.org/10.1261/rna.2309906.
15. Paek KY, Hong KY, Ryu I, Park SM, Keum SJ, Kwon OS, Jang SK. 2015. Translation initiation mediated by RNA looping. Proc Natl Acad Sci U S A 112:1041–1046. https://doi.org/10.1073/pnas.1416883112.
16. Audigier S, Guiramand J, Prado-Lourenco L, Conte C, Gonzalez-Herrera IG, Cohen-Solal C, Recasens M, Prats AC. 2008. Potent activation of FGF-2 IRES-dependent mechanism of translation during brain development. RNA 14:1852–1864. https://doi.org/10.1261/rna.790608.
17. Graber TE, Holcik M. 2007. Cap-independent regulation of gene expression in apoptosis. Mol Biosyst 3:825–834. https://doi.org/10.1039/b708867a.
18. Xue S, Tian S, Fujii K, Kladwang W, Das R, Barna M. 2015. RNA regulons in Hox 5′ UTRs confer ribosome specificity to gene regulation. Nature 517:33–38. https://doi.org/10.1038/nature14010.
19. Kim H-J, Lee H-R, Seo J-Y, Ryu HG, Lee K-H, Kim D-Y, Kim K-T. 2017. Heterogeneous nuclear ribonucleoprotein A1 regulates rhythmic synthesis of mouse Nfil3 protein via IRES-mediated translation. Sci Rep 7:42882. https://www.nature.com/articles/srep42882#supplementary-information.
20. Choi JH, Wang W, Park D, Kim SH, Kim KT, Min KT. 2018. IRES-mediated translation of cofilin regulates axonal growth cone extension and turning. EMBO J 37:e95266. https://doi.org/10.15252/embj.201695266.
21. Weingarten-Gabbay S, Elias-Kirma S, Nir R, Gritsenko AA, Stern-Ginossar N, Yakhini Z, Weinberger A, Segal E. 2016. Systematic discovery of cap-independent translation sequences in human and viral genomes. Science 351:aad4939. https://doi.org/10.1126/science.aad4939.
22. Pichon X, Wilson LA, Stoneley M, Bastide A, King HA, Somers J, Willis AE. 2012. RNA binding protein/RNA element interactions and the control of translation. Cpps 13:294–304. https://doi.org/10.2174/138920312801619475.
23. Kim JH, Paek KY, Ha SH, Cho S, Choi K, Kim CS, Ryu SH, Jang SK. 2004. A cellular RNA-binding protein enhances internal ribosomal entry site-dependent translation through an interaction downstream of the hepatitis C virus polyprotein initiation codon. Mol Cell Biol 24:7878–7890. https://doi.org/10.1128/MCB.24.18.7878-7890.2004.
24. Kim DY, Woo KC, Lee KH, Kim TD, Kim KT. 2010. hnRNP Q and PTB modulate the circadian oscillation of mouse Rev-erb alpha via IRES-mediated translation. Nucleic Acids Res 38:7068–7078. https://doi.org/10.1093/nar/gkq569.
25. Lee P-T, Chao P-K, Ou L-C, Chuang J-Y, Lin Y-C, Chen S-C, Chang H-F, Law P-Y, Loh HH, Chao Y-S, Su T-P, Yeh S-H. 2014. Morphine drives internal ribosome entry site-mediated hnRNP K translation in neurons through opioid receptor-dependent signaling. Nucleic Acids Res 42:13012–13025. https://doi.org/10.1093/nar/gku1016.
26. Xing L, Yao X, Williams KR, Bassell GJ. 2012. Negative regulation of RhoA translation and signaling by hnRNP-Q1 affects cellular morphogenesis. Mol Biol Cell 23:1500–1509. https://doi.org/10.1091/mbc.e11-10-0867.
27. Lai C-H, Huang Y-C, Lee J-C, Tseng JT-C, Chang K-C, Chen Y-J, Ding N-J, Huang P-H, Chang W-C, Lin B-W, Chen R-Y, Wang Y-C, Lai Y-C, Hung L-Y. 2017. Translational upregulation of Aurora-A by hnRNP Q1 contributes to cell proliferation and tumorigenesis in colorectal cancer. Cell Death Dis 8:e2555. https://www.nature.com/articles/cddis2016479#supplementary-information.
28. Chen HH, Yu HI, Chiang WC, Lin YD, Shia BC, Tarn WY. 2012. hnRNP Q regulates Cdc42-mediated neuronal morphogenesis. Mol Cell Biol 32:2224–2238. https://doi.org/10.1128/MCB.06550-11.
29. Kim DY, Kim W, Lee KH, Kim SH, Lee HR, Kim HJ, Jung Y, Choi JH, Kim KT. 2013. hnRNP Q regulates translation of p53 in normal and stress conditions. Cell Death Differ 20:226–234. https://doi.org/10.1038/cdd.2012.109.

30. Kim TD, Woo KC, Cho S, Ha DC, Jang SK, Kim KT. 2007. Rhythmic control of AANAT translation by hnRNP Q in circadian melatonin production. Genes Dev 21:797–810. https://doi.org/10.1101/gad.1519507.
31. Lee KH, Woo KC, Kim DY, Kim TD, Shin J, Park SM, Jang SK, Kim KT. 2012. Rhythmic interaction between Period1 mRNA and hnRNP Q leads to circadian time-dependent translation. Mol Cell Biol 32:717–728. https://doi.org/10.1128/MCB.06177-11.
32. Halstead JM, Lin YQ, Durraine L, Hamilton RS, Ball G, Neely GG, Bellen HJ, Davis I. 2014. Syncrip/hnRNP Q influences synaptic transmission and regulates BMP signaling at the Drosophila neuromuscular synapse. Biol Open 3:839–849. https://doi.org/10.1242/bio.20149027.
33. Mann F, Rougon G. 2007. Mechanisms of axon guidance: membrane dynamics and axonal transport in semaphorin signalling. J Neurochem 102:316–323. https://doi.org/10.1111/j.1471-4159.2007.04578.x.
34. Manns RPC, Cook GMW, Holt CE, Keynes RJ. 2012. Differing semaphorin 3A concentrations trigger distinct signaling mechanisms in growth cone collapse. J Neurosci 32:8554–8559. https://doi.org/10.1523/JNEUROSCI.5964-11.2012.
35. Jongbloets BC, Pasterkamp RJ. 2014. Semaphorin signalling during development. Development 141:3292–3297. https://doi.org/10.1242/dev.105544.
36. Li C, Bassell GJ, Sasaki Y. 2009. Fragile X mental retardation protein is involved in protein synthesis-dependent collapse of growth cones induced by semaphorin-3A. Front Neural Circuits 3:11. https://doi.org/10.3389/neuro.04.011.2009.
37. Aizawa H, Wakatsuki S, Ishii A, Moriyama K, Sasaki Y, Ohashi K, Sekine-Aizawa Y, Sehara-Fujisawa A, Mizuno K, Goshima Y, Yahara I. 2001. Phosphorylation of cofilin by LIM-kinase is necessary for semaphorin 3A-induced growth cone collapse. Nat Neurosci 4:367–373. https://doi.org/10.1038/86011.
38. Chiang P-W, Carpenter LE, Hagerman PJ. 2001. The 5′ untranslated region of the FMR1 message facilitates translation by internal ribosome entry. J Biol Chem 276:37916–37921. https://doi.org/10.1074/jbc.M105584200.
39. Dobson T, Kube E, Timmerman S, Krushel LA. 2008. Identifying intrinsic and extrinsic determinants that regulate internal initiation of translation mediated by the FMR1 5′ leader. BMC Mol Biol 9:89. https://doi.org/10.1186/1471-2199-9-89.
40. Ludwig AL, Hershey JWB, Hagerman PJ. 2011. Initiation of translation of the FMR1 mRNA occurs predominantly through 5′ end-dependent ribosomal scanning. J Mol Biol 407:21–34. https://doi.org/10.1016/j.jmb.2011.01.006.
41. Bochkov YA, Palmenberg AC. 2006. Translational efficiency of EMCV IRES in bicistronic vectors is dependent upon IRES sequence and gene location. Biotechniques 41:283–292. https://doi.org/10.2144/000112243.
42. Landry DM, Hertz MI, Thompson SR. 2009. RPS25 is essential for translation initiation by the Dicistroviridae and hepatitis C viral IRESs. Genes Dev 23:2753–2764. https://doi.org/10.1101/gad.1832209.
43. Wang Z, Weaver M, Magnuson NS. 2005. Cryptic promoter activity in the DNA sequence corresponding to the pim-1 5′-UTR. Nucleic Acids Res 33:2248–2258. https://doi.org/10.1093/nar/gki523.
44. Lee K-H, Kim S-H, Kim H-J, Kim W, Lee H-R, Jung Y, Choi J-H, Hong KY, Jang SK, Kim K-T. 2014. AUF1 contributes to Cryptochrome1 mRNA degradation and rhythmic translation. Nucleic Acids Res 42:3590–3606. https://doi.org/10.1093/nar/gkt1379.
45. Showkat M, Beigh MA, Andrabi KI. 2014. mTOR signaling in protein translation regulation: implications in cancer genesis and therapeutic interventions. Mol Biol Int 2014:1. https://doi.org/10.1155/2014/686984.
46. Oudard S, Medioni J, Aylllon J, Barrascourt E, Elaidi R-T, Balcaceres J, Scotte F. 2009. Everolimus (RAD001): an mTOR inhibitor for the treatment of metastatic renal cell carcinoma. Expert Rev Anticancer Ther 9:705–717. https://doi.org/10.1586/era.09.27.
47. De Wit J, De Winter F, Klooster J, Verhaagen J. 2005. Semaphorin 3A displays a punctate distribution on the surface of neuronal cells and interacts with proteoglycans in the extracellular matrix. Mol Cell Neurosci 29:40–55. https://doi.org/10.1016/j.mcn.2004.12.009.
48. Kozak M. 1989. Circumstances and mechanisms of inhibition of translation by secondary structure in eucaryotic mRNAs. Mol Cell Biol 9:5134–5142.
49. Kim SH, Lee KH, Kim DY, Kwak E, Kim S, Kim KT. 2015. Rhythmic control of mRNA stability modulates circadian amplitude of mouse Period3 mRNA. J Neurochem 132:642–656. https://doi.org/10.1111/jnc.13027.
50. Ran FA, Hsu PD, Wright J, Agarwala V, Scott DA, Zhang F. 2013. Genome engineering using the CRISPR-Cas9 system. Nat Protoc 8:2281–2308. https://doi.org/10.1038/nprot.2013.143.
51. Tom Dieck S, Kochen L, Hanus C, Heumuller M, Bartnik I, Nassim-Assir B, Merk K, Mosler T, Garg S, Bunse S, Tirrell DA, Schuman EM. 2015. Direct visualization of newly synthesized target proteins in situ. Nat Methods 12:411–414. https://doi.org/10.1038/nmeth.3319.